LETTER

doi:10.1038/nature09446

Anthrax toxins cooperatively inhibit endocytic recycling by the Rab11/Sec15 exocyst

Annabel Guichard[1], Shauna M. McGillivray[2,3]*, Beatriz Cruz-Moreno[1]*, Nina M. van Sorge[2]*, Victor Nizet[2,4] & Ethan Bier[1]

Bacillus anthracis **is the causative agent of anthrax in humans and other mammals[1,2]. In lethal systemic anthrax, proliferating bacilli secrete large quantities of the toxins lethal factor (LF) and oedema factor (EF), leading to widespread vascular leakage and shock. Whereas host targets of LF (mitogen-activated protein-kinase kinases) and EF (cAMP-dependent processes)[3] have been implicated in the initial phase of anthrax[1,2], less is understood about toxin action during the final stage of infection. Here we use *Drosophila melanogaster* to identify the Rab11/Sec15 exocyst, which acts at the last step of endocytic recycling, as a novel target of both EF and LF. EF reduces levels of apically localized Rab11 and indirectly blocks vesicle formation by its binding partner and effector Sec15 (Sec15–GFP), whereas LF acts more directly to reduce Sec15–GFP vesicles. Convergent effects of EF and LF on Rab11/Sec15 inhibit expression of and signalling by the Notch ligand Delta and reduce DE-cadherin levels at adherens junctions. In human endothelial cells, the two toxins act in a conserved fashion to block formation of Sec15 vesicles, inhibit Notch signalling, and reduce cadherin expression at adherens junctions. This coordinated disruption of the Rab11/Sec15 exocyst by anthrax toxins may contribute to toxin-dependent barrier disruption and vascular dysfunction during *B. anthracis* infection.**

B. anthracis, the aetiological agent of anthrax, secretes three factors that are required for systemic virulence[1–3]: the toxic enzymatic moieties LF and EF, and protective antigen (PA), which promotes entry of LF and EF into host cells. LF is a zinc metalloprotease that cleaves and inactivates most human mitogen-activated protein-kinase kinases (MAPKKs)[4,5], and EF is a potent calmodulin-dependent adenylate cyclase[6]. It has been speculated that additional host targets may contribute to mediating the lethal effects of anthrax toxins[7] and interactions between the two toxins remain poorly understood.

We chose *D. melanogaster* as a model system to identify new candidate pathways involved in anthrax pathogenesis. LF and EF act on conserved signalling components, MAPKKs and PKA, respectively, when expressed directly within the cells of transgenic flies, bypassing the need for PA-mediated endocytosis[8]. Here we report that strong expression of either LF or EF in the larval wing primordium also produces new, unexpected phenotypes. These phenotypes, including wing notching and thickened veins (Supplementary Fig. 1a–c and Supplementary Fig. 2a), are typical of mutants in the Notch signalling pathway and were strongest for EF when using the same *GAL4* driver (for example, Fig. 1b, c and h, i). Consistent with these adult phenotypes, high-level expression of either toxin greatly reduced expression of the Notch target genes *wg* and *cut* (Supplementary Fig. 1d–i). We also observed potent dose-sensitive genetic interactions between mutations in Notch pathway components and the expression of LF (Supplementary Fig. 2b–f) or EF (Supplementary Fig. 2g–n).

An important unresolved issue is whether LF and EF, which are both required individually for the pathogenicity of *B. anthracis*, also interact in some concerted fashion[9]. We tested for toxin synergy by co-expressing them with a weak ubiquitous wing-specific *GAL4* (*wkG4*) driver. Expression of LF alone produced no obvious phenotype (Fig. 1b, compare to wild type in a). Similarly, expression of only EF resulted in mild occasional notching of the wing margin (Fig. 1c), although it also caused an unrelated phenotype consisting of small wings with altered vein spacing. When EF and LF were co-expressed with this *GAL4* driver, however, strong and penetrant wing margin notching phenotypes were superimposed on the EF patterning phenotype (Fig. 1d). Correspondingly, expression of the Notch target gene *wg* (Fig. 1a–d, lower panels) and a Notch reporter construct (not shown) were greatly reduced in LF+EF wing discs. Synergy between LF and EF was also observed using other drivers, such as a strong ubiquitous *GAL4* driver (*stgG4*) (Fig. 1h–j) and the *dpp-GAL4* driver (*dppG4*) (data not shown).

These initial phenotypic observations led us to examine the mechanisms underlying the Notch inhibitory effects of the anthrax toxins. Both LF (Fig. 1e, f) and EF (Fig. 1e, g) greatly reduced levels of the Notch ligand Delta (Dl) at the apical surface of wing discs, which we confirmed by selective staining for extracellular Dl expression (Supplementary Fig. 3a–c), and modestly decreased apical levels of Notch (Supplementary Fig. 3g–i). EF also significantly reduced surface expression of a second Notch ligand, Serrate (Supplementary Fig. 3d, e). We conclude that both LF and EF inhibit trafficking of Dl to the apical cell surface, diminishing Notch signalling.

Activation of Dl requires initial cell surface expression followed by endocytosis and recycling (reviewed in ref. 10), targeting it to the adherens junction, where it engages the Notch receptor[11]. Small GTPases from the Rab family mediate specific steps of this process[12]. We expressed dominant-negative forms of each of the *Drosophila* Rab proteins (Rab(DN))[13] and identified a single dominant-negative factor, Rab11(DN), which produced phenotypes virtually identical to those caused by EF (Fig. 1i, k, Supplementary Fig. 4b, c and Supplementary Table 1). Reciprocally, we co-expressed wild-type forms of each Rab with EF to determine whether increasing their dosage could rescue the Notch-like EF phenotype and found that only Rab11 could suppress EF activity (Fig. 1l, m, compare to i; Supplementary Table 1). Consistent with Rab11 mediating the inhibition of Notch signalling by EF, co-expression of Rab11(DN) with EF greatly enhanced its wing phenotypes (Fig. 1n) and Rab11(DN), like EF, could synergize with LF to produce a stronger phenotype (Fig. 1o, similar to j). Rab11(DN) also mimicked the effect of EF in blocking Dl trafficking to the cell surface (Supplementary Fig. 5d–f). A similar role of Rab11 in recycling endocytosed Dl to the apical cell surface has been demonstrated during sensory organ precursor cell development in *Drosophila*[11,14].

The endogenous Rab11 protein is distributed as small grainy particles just below the apical plasma membrane in wild-type wing discs[11] (Fig. 2a). In EF-expressing discs, the level of apical Rab11 expression was greatly diminished (Fig. 2b) and ectopic Rab11-positive vesicles

[1]Section of Cell and Developmental Biology, University of California, San Diego, 9500 Gilman Drive, La Jolla, California 92093-0349, USA. [2]Department of Pediatrics, University of California, San Diego, 9500 Gilman Drive, La Jolla, California 92093-0687, USA. [3]Department of Biology, Texas Christian University, 2800 South University Drive, Fort Worth, Texas 76129, USA. [4]Skaggs School of Pharmacy & Pharmaceutical Sciences, University of California, San Diego, 9500 Gilman Drive, La Jolla, California 92093-0687, USA.
*These authors contributed equally to this work.

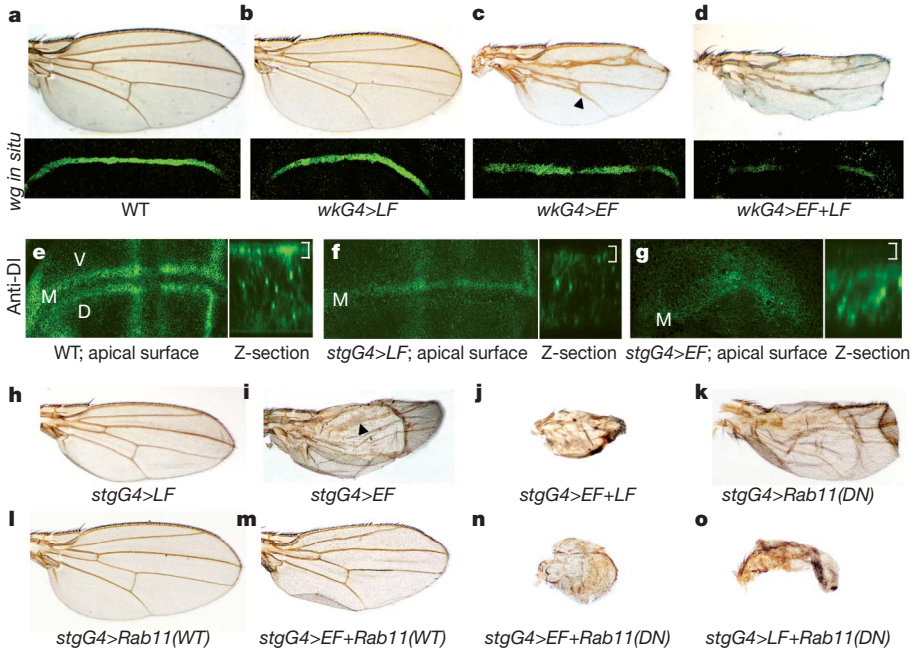

Figure 1 | LF and EF synergistically inhibit Notch signalling. **a**–**d**, Wings (upper panels) and corresponding *wg* expression in wing imaginal discs (bottom panels) of the following genotypes: **a**, wild-type (WT); **b**, *wkG4>LF2X* (*wkG4* refers to the *1348-GAL4* driver); **c**, *wkG4>EF* (wing has anterior/posterior patterning phenotype superimposed on thickened veins (arrowhead) and an occasional small notch at the wing margin); **d**, *wkG4>LF2X+EF* (*LF2X* refers to two copies of the *UAS-LF* transgene). **e**–**g**, Reticular pattern of Dl staining in wing discs with accompanying Z-sections. The *stgG4* driver (*MS1096GAL4*) is expressed at higher levels on the dorsal (D) surface than on the ventral (V) surface. **e**, Wild-type Dl expression has both cell surface (bracket) and vesicle-like intracellular components, and is expressed along the future margin (M) in two parallel lines as well as in vein primordia (which intersect the margin in perpendicular stripes). **f**, *stgG4>LF* (here, and in all subsequent panels, *LF* refers to three copies of the *UAS-LF* transgene). **g**, *stgG4>EF*. **h**–**o**, Wings of the following genotypes: **h**, *stgG4>LF*; **i**, *stgG4>EF* (arrowhead indicates thickened veins); **j**, *stgG4>LF+EF*; **k**, *stgG4>Rab11(DN)*; **l**, *stgG4>Rab11(WT)*; **m**, *stgG4>EF+Rab11(WT)*; **n**, *stgG4>EF+Rab11(DN)*; **o**, *stgG4>LF+Rab11(DN)*.

appeared in basolateral areas of the cytoplasm (quantified in Supplementary Table 2). This finding indicates that EF acts, at least in part, by reducing the amount and/or altering the distribution of the Rab11 GTPase. Because Rab11 has been implicated in targeting other proteins to the adherens junction in addition to Notch signalling components[15], we examined the expression of several adherens junction proteins. In wild-type wing discs, the homophylic adhesion molecule DE-cadherin (DECad) is expressed at points of cell–cell contact (Fig. 2d), where it co-localizes with Dl (Supplementary Fig. 5a–c). In contrast, EF precipitously reduced DECad expression at the adherens junction (Fig. 2e), mimicking the effect of inhibiting Rab11 function (Fig. 2f and Supplementary Fig. 6a, b). This downregulation of DECad by EF could be partially rescued by co-expression with wild-type Rab11 (Supplementary Fig. 5g–i). Similar, albeit less pronounced, reductions were observed for the adherens junction proteins α-Catenin and β-Catenin (Supplementary Fig. 6d, e and g, h, respectively); however, Discs Large (Dlg) expression was unaltered (Supplementary Fig. 6j, k), indicating that EF acts selectively and does not lead to gross disruption of adherens junction integrity per se.

As Rab11 interacts with its effector Sec15 to initiate formation of the exocyst complex, thereby leading to fusion of vesicles from the recycling endosome with the plasma membrane (reviewed in ref. 12), we examined the effect of EF on expression of a *Drosophila* Sec15–GFP fusion protein construct[11]. Sec15–GFP expression has two staining components (Fig. 2g): large round structures near the cell surface and diffuse cytoplasmic staining. Vesicular Sec15–GFP, which corresponds to a late endocytic compartment poised to fuse with the plasma membrane[11,16–18], co-localized with Rab11 (Fig. 2j and Supplementary Fig. 7a), consistent with the known interaction of these two proteins in the exocyst complex[11,15,19]. Expression of EF virtually abolished large Sec15–GFP vesicles (Fig. 2h), and the few that remained were typically smaller than those in wild-type discs and did not co-label as strongly with Rab11 (Supplementary Fig. 7a, b). In contrast, the uniform cytoplasmic component of Sec15–GFP staining was largely unaltered by EF. EF probably blocks formation of large Sec15–GFP vesicles indirectly, through its effect on Rab11, because inhibition of Rab11 by Rab11(DN) (Fig. 2i) or by RNA-mediated interference (RNAi) (data not shown) had the same effect. Furthermore, co-expression of wild-type Rab11 with EF fully rescued punctate Sec15–GFP expression (Fig. 2k and Supplementary Fig. 8a–c).

Because EF and LF interact synergistically in the wing and both toxins reduce access of Dl to the cell surface, we tested whether LF acted at the same recycling step as EF. Although LF did not appreciably alter Rab11 staining (Fig. 2c) it, like EF, nearly eliminated large Sec15–GFP vesicles (Fig. 2l) and residual small Sec15–GFP vesicles no longer strongly co-labelled with Rab11 (Supplementary Fig. 7a, c). In contrast to EF, however, the loss of Sec15–GFP staining was only weakly rescued by co-expression with wild-type Rab11 (Supplementary Fig. 8e, f, compare to b, c for EF). LF also reduced levels of DECad at the apical cell surface (Supplementary Fig. 6a–c), although not as strongly as EF. Consistent with Sec15 being a mediator of LF Notch inhibitory activity, knockdown of endogenous *sec15* function by RNAi caused Notch-like phenotypes in the wing (Supplementary Fig. 9b, d), although overexpression of wild-type *sec15* had no effect (Supplementary Fig. 9a, c). We conclude that LF and EF converge to inhibit two interacting components of the Rab11/Sec15 exocyst, resulting in reduced Notch signalling and weakened adherens junctions.

We next asked whether EF and LF could disrupt function of the well-conserved Rab11/Sec15 exocyst and its downstream effectors Notch and cadherins in mammalian systems. Established models of endothelial cell function were selected as Notch signalling has a central role in vascular remodelling (reviewed in ref. 20), and cadherins are essential for maintaining vascular integrity[21]. We transfected a rat Sec15–GFP construct into human brain microvascular endothelial cells (hBMECs) to visualize the exocyst and observed large vesicles (Fig. 3a, d) similar to those in *Drosophila* wing discs (for example, Fig. 2g), yeast[17] and various mammalian cell types[18]. As in *Drosophila*, treatment with either EF toxin (EF+PA) (Fig. 3b, h) or LF toxin (LF+PA) (Fig. 3c) greatly

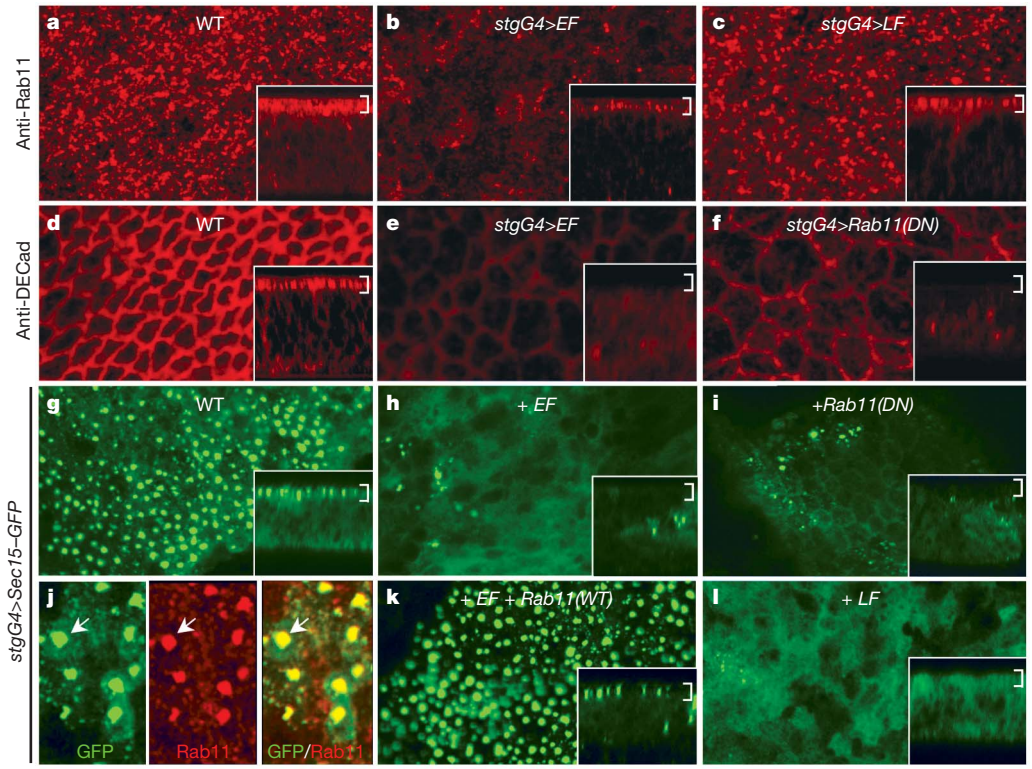

Figure 2 | LF and EF inhibit Rab11/Sec15-dependent recycling. **a**–**c**, Endogenous Rab11 expression in wing imaginal discs detected by immunofluorescence. Insets are Z-sections from regions of the same discs in these and other panels (brackets indicate the cell surface). **a**, Wild type. **b**, *stgG4>EF*. **c**, *stgG4>LF*. **d**–**f**, DECad expression detected by immunofluorescence. **d**, Wild type. DECad and Dl co-stain in a net-like pattern at points of cell–cell contact (Supplementary Fig. 5a–c). **e**, *stgG4>EF*. **f**, *stgG4>Rab11(DN)*. **g**–**l**, Expression of a *UAS-Sec15–GFP* construct driven by the *stgG4* driver. **g**, Wild-type wing disc expressing *stgG4>Sec15–GFP* in large vesicles beneath the cell surface. **h**, *stgG4>EF+Sec15–GFP*. **i**, *stgG4>Rab11(DN)+Sec15–GFP* (vesicular Sec15–GFP expression is similarly dependent on *Rab11 = Sec4* function in yeast[17]). **j**, High-magnification view of Sec15–GFP and Rab11 co-localization in a wild-type wing disc. Left panel, Sec15–GFP (green). Middle panel, Rab11 (red). Right panel, overlap between Sec15–GFP and Rab11 (yellow). Arrows indicate one example of co-localization. **k**, *stgG4>EF+Rab11(WT)+Sec15–GFP*. **l**, *stgG4>LF+Sec15–GFP*. Staining differences are quantified in Supplementary Table 2.

reduced the number and size of the Sec15–GFP vesicles. Moreover, in the case of EF toxin, co-transfection of cells with human RAB11–RFP rescued the formation of large Sec15–GFP vesicles (compare Fig. 3h with i). Mirroring other systems, Rab11 and Sec15 co-localized, both in untreated (Fig. 3e–g) and in EF-treated endothelial cells rescued with RAB11–RFP (Fig. 3i–k). We conclude that the EF and LF toxins function similarly in human and *Drosophila* cells to disrupt formation of the Rab11/Sec15 exocyst.

Looking downstream of the exocyst, we found that treatment with EF toxin disrupted the strong and uninterrupted pan-cadherin (pCAD) expression found at points of cell–cell contact in untreated monolayers of hBMECs (compare Fig. 3b, h with a, d), in primary human dermal microvascular endothelial cells (hDMECs; compare Fig. 3m with l; Supplementary Fig. 10a, b), and in primary human lung microvascular endothelial cells (hMVEC-Ls; Supplementary Fig. 11a, b). LF toxin had no clear effect on pCAD in hBMECs (Fig. 3c), although levels were moderately reduced in hDMECs (Supplementary Fig. 10c), which form more regular borders than hBMECs.

We also examined the effect of anthrax toxins on Notch signalling in mammalian cells. hBMECs were infected with wild-type *B. anthracis* Sterne bacteria, which express both EF and LF, or isogenic mutant bacteria lacking EF (ΔEF), LF (ΔLF), or both toxins (ΔLF+EF or ΔpXO1)[22]. Bacterial anthrax toxin production inhibited hBMEC expression of the Notch target gene *HES1* (Fig. 3n; quantified in Supplementary Fig. 12a) and *RBPJ* (Supplementary Fig. 12b), with EF exerting the dominant effect. Notch-dependent regulation of *HES1* in hBMECs was confirmed using the γ-secretase inhibitor DBZ (Fig. 3n). In addition, EF toxin treatment of hDMECs or hMVEC-Ls triggered formation of large and misshapen intracellular vesicles of the endothelial-specific Notch ligand Delta-Like 4 (DLL4) (compare Fig. 3m with l and Supplementary Fig. 11a with b) as observed in *Drosophila* (Fig. 1e–g).

Because previous studies have described the effect of anthrax toxins on vascular leakage and pulmonary oedema[9,23,24], we analysed endothelial barrier integrity using *in vitro* and *in vivo* assays during infection. Exposure to wild-type *B. anthracis* increased the permeability of hBMEC transwell monolayers, an effect principally dependent on EF activity (Fig. 3o). Similarly, purified EF toxin induced dose-dependent hBMEC permeability in the same assay (Supplementary Fig. 12c). Next, individual mice were infected subcutaneously in adjacent locations with wild-type and mutant strains of *B. anthracis*[22], followed 6 h later by intravenous injection of Evans blue dye (Miles assay[25,26]). Wild-type *B. anthracis* induced severe vascular effusion at the site of injection (Fig. 3p), and this effect was greatly attenuated in ΔEF mutant bacteria, but only modestly so in ΔLF mutants (Fig. 3p, q). Similarly in the lung, wild-type *B. anthracis* induced pulmonary oedema, indicative of pulmonary endothelial barrier dysfunction, and this effect was also abrogated in ΔEF mutant bacteria (Supplementary Fig. 11c, d).

In summary, LF and EF toxins interact synergistically in *Drosophila* to block Rab11/Sec15-dependent endocytic recycling, resulting in reduced Notch signalling and cadherin-dependent adhesion at the adherens junction, and these toxins produce very similar effects in mammalian cells. Failure to target proteins to the adherens junction may contribute to the loss of endothelial barrier integrity in EF-toxin-treated cells and to the toxin-dependent vascular effusion caused *in vivo* during *B. anthracis* infection (see summary scheme in Fig. 3r). The reduction in Dl/Notch levels in response to anthrax toxin treatment requires further analysis with respect to potential consequences

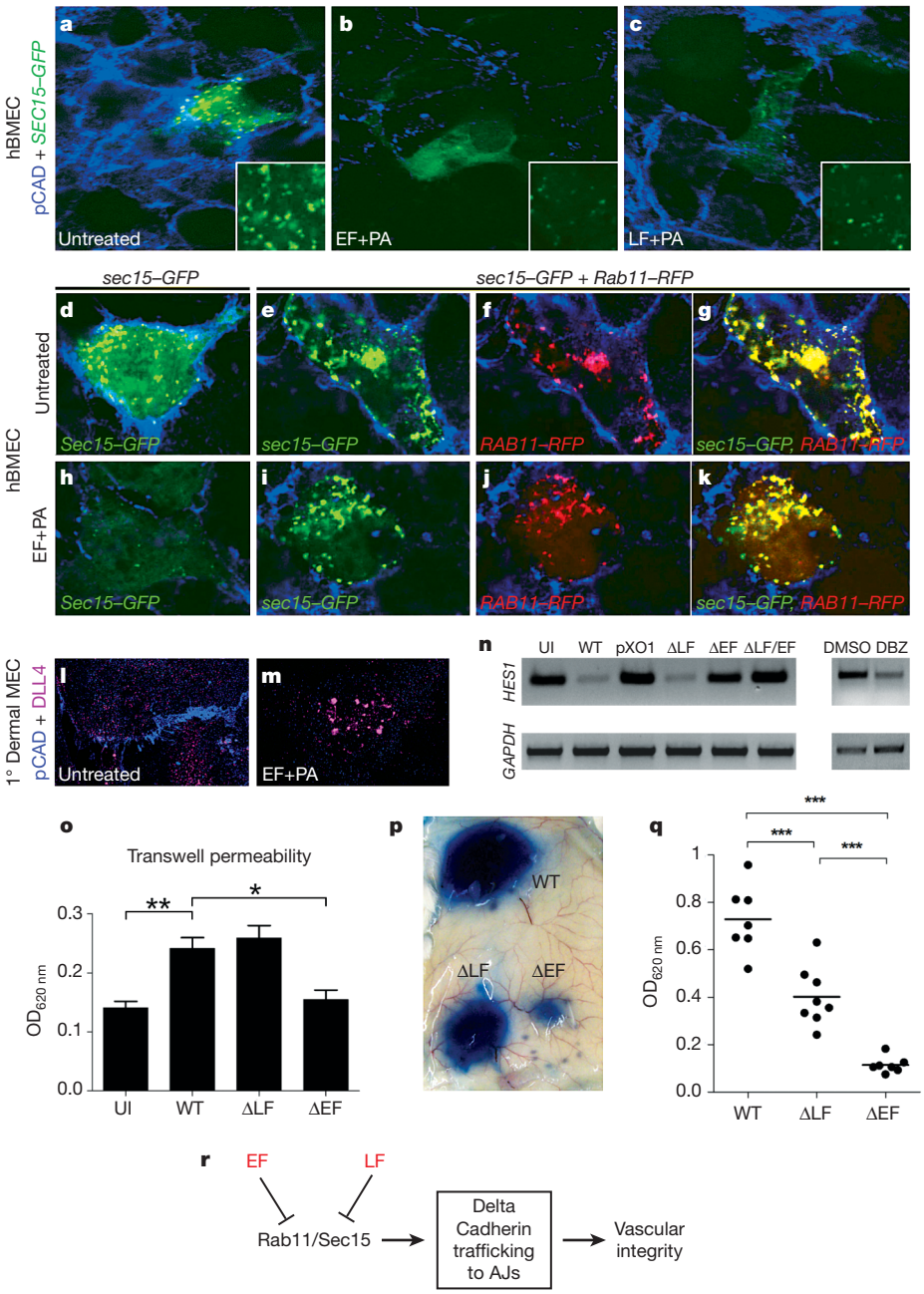

Figure 3 | Conserved activity of anthrax toxins in mammals. **a**–**c**, Pan-cadherin (pCAD) staining (blue) in hBMECs transfected with a human *SEC15–GFP* construct (green). **a**, Untreated cells. **b**, Cells treated with EF toxin (3 μg EF and 6 μg PA) for 24 h. **c**, Cells treated with LF toxin (3 μg LF and 6 μg PA) for 24 h. Treatment with doses ranging from 0.3 μg to 3 μg gave similar results. Staining differences are quantified in the legend of Supplementary Table 2. **d**–**k**, Rescue of Sec15–GFP (green) expression by Rab11–RFP (red) in EF-toxin-treated hBMECs. **d**–**g**, Untreated cells, and **h**–**k**, cells treated with 0.3 μg EF and 0.6 μg PA. **d**, **h**, Cells transfected with *Sec15–GFP* alone. **e**–**g**, **i**–**k**, Cells co-transfected with *sec15–GFP* and wild-type *RAB11–RFP*. Cells in panels **d**–**k** were also stained for pCAD (blue). **l**, **m**, Expression of pCAD (blue) and DLL4 (magenta) in untreated hDMECs (**l**), or after treatment with 1 μg EF and 2 μg PA (**m**). **n**, Semi-quantitative analysis of *HES1* and *GAPDH* RNA expression in hBMECs. First set of lanes, hBMECs infected with *B. anthracis* or isogenic mutants. UI, uninfected control; WT, *B. anthracis* Sterne bacteria; ΔpX01, *B. anthracis* lacking the pX01 plasmid; ΔLF, *B. anthracis* with deletion of LF; ΔEF, *B. anthracis* with deletion of EF; ΔLF/ΔEF, *B. anthracis* with deletion of both LF and EF. Second set of lanes, effect of the γ-secretase inhibitor DBZ (2 μM) or vehicle control (dimethyl sulphoxide (DMSO)) on *HES1* expression in hBMECs. **o**, Transwell permeability assay of hBMECs grown to confluence in a transwell chamber and infected with *B. anthracis* wild-type or isogenic toxin mutants. Leakage across the monolayer was determined 6 h later by measuring Evans blue leakage to the bottom chamber at $OD_{620\,nm}$. Abbreviations for genotypes of bacteria are as in panel **n**. *, $P < 0.05$; **, $P < 0.01$. Mean and standard deviation (represented by error bars) of a representative experiment are shown. **p**, Vascular effusion in response to subcutaneous infection with *B. anthracis* (wild-type *B. anthracis*) or isogenic toxin mutants ΔLF or ΔEF. Effusion was visualized by Evans blue dye leakage. **q**, Quantification of vascular permeability shown in Fig. 3p. ***, $P < 0.001$. **r**, Proposed schematic model for the convergent activity of EF and LF on the exocyst. EF reduces Rab11 levels/activity, which indirectly inhibits formation of Sec15 exocyst complexes, whereas LF acts more directly on Sec15. The combined effect of these two toxins is to reduce cell surface expression of the Notch ligand Dl and cadherins at adherens junctions (AJs), and possibly other adherens junction proteins involved in cell–cell adhesion and barrier maintenance, thereby compromising vascular integrity.

on vascular integrity, which could be direct (for example, mediated by Notch-dependent regulation of factors such as VEGF or by Dl–Notch adhesion) or indirect (for example, mediated by Notch-dependent regulation of cytokine production). The precise mechanisms by which EF and LF cooperatively inhibit Rab11/Sec15 function remain to be elucidated. EF-mediated cAMP production could act on either or both of two known effectors, PKA and Epac, both of which have connections to Rab11 regulation[27,28]. LF may function via cleavage and inactivation of its known MAPKK targets or act on novel targets. It is also unclear why EF has consistently stronger effects than LF in both flies and vertebrates, as they both converge on the exocyst. It may be that Rab11 has additional partners that act in parallel to Sec15. Alternatively, LF may block only a subset of Sec15 functions or may exert competing effects on the exocyst mediated by opposing actions of different MAPKKs or as yet unidentified targets. Future genetic dissection of these impinging pathways will be required to distinguish between these possibilities. Finally, it may be fruitful to examine whether the mammalian exocyst and its downstream effectors could also be targets of other microbial virulence factors known to increase cAMP levels, inhibit MAPKK signalling, or disrupt host barrier integrity.

METHODS SUMMARY

***Drosophila* genetics.** Transgenic lines UAS-LF2X/FM7, UAS-LF3X/FM7 and UAS-EF UAS-Flp/TM3 were described previously[8]. UAS-Sec15–GFP was provided by H. Bellen. UAS-Rab and GAL4 lines were obtained from the Bloomington *Drosophila* stock centre. The UAS-*sec15* RNAi stock was obtained from the Vienna Drosophila RNAi Centre (VDRC).

Immunofluorescence on imaginal discs. Imaginal disc staining involved the following antibodies: anti-Dl (clone C594.9B-c; A. Parks), rat anti-Rab11 (R. Cohen) and rat anti-Serrate (K. Irvine). Other antibodies were obtained from the Developmental Studies Hydridoma Bank (DSHB): anti-Cut (2B10-c), anti-DECad (DCAD2), anti-α-catenin (DCAT-1), anti-β-Catenin (N2 7A1), anti-Discs Large (DLG1) and anti-NotchECD (C458.2H). *In situ* hybridization on wing discs was performed as described[29].

hBMEC, hDMEC and hMVEC-L experiments. hBMECs[30] were infected with *B. anthracis* Sterne ($pXO1^+$, $pXO2^-$) or isogenic mutants[22] and RNA was collected 6 h later[30] for semi-quantitative PCR and quantitative PCR. For immunofluorescence, hBMECs were transfected using 0.5 μg of DNA (rat *Sec15–GFP*[18] plasmid was provided by C. Mitchell and human *RAB11-RFP* plasmid was a gift from M. Colombo) plus 2 μl Fugene (Roche). Purified EF+PA or LF+PA (S. Leppla) were added for 24 h and fixed cells were stained using anti-pan-cadherin (pCAD) (Abcam, ab6528) or anti-Dll4 antibodies (Lifespan). For transwell assays, cells were grown on collagenized transwells (Transwell-COL) for 7 days. hDMECs (Lonza CC-2543) or hMVEC-Ls (Lonza, CC-2527) were treated with purified EF or LF toxin, fixed and stained as described earlier for hBMECs except that hMVEC-Ls were treated with EF toxin for 48 h. Vascular permeability in the skin was assessed using the Miles assay[25,26].

Full Methods and any associated references are available in the online version of the paper at www.nature.com/nature.

Received 12 April; accepted 23 August 2010.

1. Mourez, M. Anthrax toxins. *Rev. Physiol. Biochem. Pharmacol.* **152,** 135–164 (2004).
2. Tournier, J. N., Quesnel-Hellmann, A., Cleret, A. & Vidal, D. R. Contribution of toxins to the pathogenesis of inhalational anthrax. *Cell. Microbiol.* **9,** 555–565 (2007).
3. Lacy, D. B. & Collier, R. J. Structure and function of anthrax toxin. *Curr. Top. Microbiol. Immunol.* **271,** 61–85 (2002).
4. Duesbery, N. S. *et al.* Proteolytic inactivation of MAP-kinase-kinase by anthrax lethal factor. *Science* **280,** 734–737 (1998).
5. Vitale, G. *et al.* Anthrax lethal factor cleaves the N-terminus of MAPKKs and induces tyrosine/threonine phosphorylation of MAPKs in cultured macrophages. *Biochem. Biophys. Res. Commun.* **248,** 706–711 (1998).
6. Leppla, S. H. Anthrax toxin edema factor: a bacterial adenylate cyclase that increases cyclic AMP concentrations of eukaryotic cells. *Proc. Natl Acad. Sci. USA* **79,** 3162–3166 (1982).
7. Moayeri, M. & Leppla, S. H. The roles of anthrax toxin in pathogenesis. *Curr. Opin. Microbiol.* **7,** 19–24 (2004).
8. Guichard, A., Park, J. M., Cruz-Moreno, B., Karin, M. & Bier, E. Anthrax lethal factor and edema factor act on conserved targets in *Drosophila*. *Proc. Natl Acad. Sci. USA* **103,** 3244–3249 (2006).
9. Pezard, C., Berche, P. & Mock, M. Contribution of individual toxin components to virulence of *Bacillus anthracis*. *Infect. Immun.* **59,** 3472–3477 (1991).
10. Fortini, M. E. & Bilder, D. Endocytic regulation of Notch signaling. *Curr. Opin. Genet. Dev.* **19,** 323–328 (2009).
11. Jafar-Nejad, H. *et al.* Sec15, a component of the exocyst, promotes notch signaling during the asymmetric division of *Drosophila* sensory organ precursors. *Dev. Cell* **9,** 351–363 (2005).
12. Wu, H., Rossi, G. & Brennwald, P. The ghost in the machine: small GTPases as spatial regulators of exocytosis. *Trends Cell Biol.* **18,** 397–404 (2008).
13. Zhang, J. *et al.* Thirty-one flavors of *Drosophila* rab proteins. *Genetics* **176,** 1307–1322 (2007).
14. Emery, G. *et al.* Asymmetric Rab 11 endosomes regulate delta recycling and specify cell fate in the *Drosophila* nervous system. *Cell* **122,** 763–773 (2005).
15. Langevin, J. *et al.* *Drosophila* exocyst components Sec5, Sec6, and Sec15 regulate DE-Cadherin trafficking from recycling endosomes to the plasma membrane. *Dev. Cell* **9,** 365–376 (2005).
16. Guo, W., Roth, D., Walch-Solimena, C. & Novick, P. The exocyst is an effector for Sec4p, targeting secretory vesicles to sites of exocytosis. *EMBO J.* **18,** 1071–1080 (1999).
17. Salminen, A. & Novick, P. J. The Sec15 protein responds to the function of the GTP binding protein, Sec4, to control vesicular traffic in yeast. *J. Cell Biol.* **109,** 1023–1036 (1989).
18. Zhang, X. M., Ellis, S., Sriratana, A., Mitchell, C. A. & Rowe, T. Sec15 is an effector for the Rab11 GTPase in mammalian cells. *J. Biol. Chem.* **279,** 43027–43034 (2004).
19. Wu, S., Mehta, S. Q., Pichaud, F., Bellen, H. J. & Quiocho, F. A. Sec15 interacts with Rab11 via a novel domain and affects Rab11 localization *in vivo*. *Nature Struct. Mol. Biol.* **12,** 879–885 (2005).
20. Roca, C. & Adams, R. H. Regulation of vascular morphogenesis by Notch signaling. *Genes Dev.* **21,** 2511–2524 (2007).
21. Dejana, E., Tournier-Lasserve, E. & Weinstein, B. M. The control of vascular integrity by endothelial cell junctions: molecular basis and pathological implications. *Dev. Cell* **16,** 209–221 (2009).
22. Janes, B. K. & Stibitz, S. Routine markerless gene replacement in *Bacillus anthracis*. *Infect. Immun.* **74,** 1949–1953 (2006).
23. Firoved, A. M. *et al.* *Bacillus anthracis* edema toxin causes extensive tissue lesions and rapid lethality in mice. *Am. J. Pathol.* **167,** 1309–1320 (2005).
24. Kuo, S. R. *et al.* Anthrax toxin-induced shock in rats is associated with pulmonary edema and hemorrhage. *Microb. Pathog.* **44,** 467–472 (2007).
25. Gozes, Y., Moayeri, M., Wiggins, J. F. & Leppla, S. H. Anthrax lethal toxin induces ketotifen-sensitive intradermal vascular leakage in certain inbred mice. *Infect. Immun.* **74,** 1266–1272 (2006).
26. Tessier, J. *et al.* Contributions of histamine, prostanoids, and neurokinins to edema elicited by edema toxin from *Bacillus anthracis*. *Infect. Immun.* **75,** 1895–1903 (2007).
27. Balzac, F. *et al.* E-cadherin endocytosis regulates the activity of Rap1: a traffic light GTPase at the crossroads between cadherin and integrin function. *J. Cell Sci.* **118,** 4765–4783 (2005).
28. Silvis, M. R. *et al.* Rab11b regulates the apical recycling of the cystic fibrosis transmembrane conductance regulator in polarized intestinal epithelial cells. *Mol. Biol. Cell* **20,** 2337–2350 (2009).
29. Kosman, D. *et al.* Multiplex detection of RNA expression in *Drosophila* embryos. *Science* **305,** 846 (2004).
30. van Sorge, N. M. *et al.* Anthrax toxins inhibit neutrophil signaling pathways in brain endothelium and contribute to the pathogenesis of meningitis. *PLoS ONE* **3,** e2964 (2008).

Supplementary Information is linked to the online version of the paper at www.nature.com/nature.

Acknowledgements We thank A. Kurciyan for help in analysing the effects of expressing wild-type and dominant-negative forms of Rab in *Drosophila*, A. Cooper and members of the E.B. and V.N. laboratories and H. Bellen for comments on the manuscript and suggestions. We thank S. Leppla for providing purified preparations of LF, EF and PA, S. Stibitz for *B. anthracis* mutants, and the following investigators for providing antibodies: R. Cohen (anti-Rab11), A. Parks (anti-Dl), K. Irvine (anti-Serrate) and J. Collier (anti-LF). Support for these studies was provided by National Institutes of Health (NIH) R01 grants AI070654 and NS29870 (E.B.), AI077780 (V.N.), an IRACDA NIH postdoctoral fellowship GM068524 (S.M.M.) and a Biomedical Research Fellowship from The Hartwell Foundation (S.M.M.).

Author Contributions All authors participated in designing the experiments. A.G. and B.C.-M. carried out the *Drosophila* experiments. S.M.M. and N.M.v.S. carried out the experiments with vertebrate cells and mice. E.B. wrote the manuscript with all other authors providing significant input.

Author Information Reprints and permissions information is available at www.nature.com/reprints. The authors declare no competing financial interests. Readers are welcome to comment on the online version of this article at www.nature.com/nature. Correspondence and requests for materials should be addressed to E.B. (ebier@ucsd.edu).

METHODS

***Drosophila* genetics.** Transgenic lines UAS-LF2X/FM7, UAS-LF3X/FM7 and UAS-EF UAS-Flp/TM3 were described previously[8]. UAS-Sec15–GFP was provided by H. Bellen. Wild-type UAS-Rab11 and UAS-Rab11(DN), as well as all UAS-Rab transgenic lines, generated by H. Bellen and M. Scott, were obtained from the Bloomington *Drosophila* stock centre. The UAS-*sec15* RNAi stock is from VDRC (#35161). GAL4 drivers included: *stgG4*, *MS1096-GAL4*; *wkG4*, *1348-GAL4*; *L2G4*, *E-GAL4*; *vgG4*, *dppG4* and *brkG4* have been described previously[31,32] and are available from the Bloomington *Drosophila* stock or can be obtained on request.

Immunofluorescence on imaginal discs. Immunostaining of imaginal discs was performed according to standard protocols, using the following antibodies: anti-Dl (clone C594.9B-c was provided by A. Parks and used at 1:1,000), anti-*Drosophila* Rab11 antibody (a gift from R. Cohen, used at 1:500), anti-Serrate antibodies (provided by K. Irvine, used at 1:1,000). Other antibodies were obtained from DSHB: anti-Cut (clone 2B10-c, 1:100), anti-DECad (DCAD2, 1:500), anti-α-Catenin (D-CAT1, 1:20), anti-β-Catenin (Armadillo, clone N2 7A1, 1:20), anti-Discs Large (DLG1, 1:20) and anti-NotchEC (C458.2H, 1:500). *In situ* hybridization on wing discs was performed using a digoxigenin-labelled *wg* antisense probe as described previously for fluorescent detection[29] and for histochemical staining[33].

hBMEC, hDMEC and hMVEC-L experiments. hBMECs[30] were infected with *B. anthracis* Sterne ($pXO1^+$, $pXO2^-$) or isogenic mutants ΔpXO1, ΔLF, ΔEF, or ΔLF/ΔEF[22] and RNA was collected 6 h later as described previously[30]. Semi-quantitative PCR was performed using 26 cycles and qPCR was performed using iQ SYBR Green supermix (BioRad). For immunofluorescence, hBMECs were treated with indicated amounts of purified EF+PA or LF+PA (provided by S. Leppla) for 24 h and stained using mouse anti-pan-cadherin antibody (pCAD) (Abcam, ab6528, 1:100) or anti-DLL4 antibodies (Lifespan, LS-C19035) and appropriate secondary antibodies. hBMECs were transfected with *Sec15–GFP* plasmid (provided by C. Mitchell) and/or *RAB11–RFP* plasmid (a gift from M. Colombo) using 0.5 μg of DNA and 2 μl Fugene (Roche). Forty hours after transfection, purified EF+PA or LF+PA were added to the wells and cells were fixed and stained 24 h later. For transwell assays, cells were seeded on collagenized transwells (Transwell-COL; Corning-Costar) and grown for 7 days at 37 °C with 5% CO_2. Cells were infected for 6 h with bacteria or treated with indicated amounts of EF toxin for 24 h. 0.4% Evans blue was added to the upper chamber and leakage was quantified by measuring the colour change in the bottom chamber containing Hank's buffered salt solution (HBSS) at 620 nm. For DBZ treatment, hBMECs were treated with a final concentration of 2 μM DBZ or vehicle control (DMSO) for 6 h. For transwell assays, cells were seeded on collagenized transwells (Transwell-COL) and grown for 7 days. Cells were infected for 6 h with bacteria or treated with indicated amounts of EF toxin for 24 h. 0.4% Evans blue was added to the upper chamber and leakage was measured at 620 nm. hDMECs (Lonza CC-2543) or hMVEC-Ls (Lonza CC-2527) were treated with purified EF or LF toxin, fixed and stained as described earlier for hBMECs except that hMVEC-Ls were treated with EF toxin for 48 h.

Vascular permeability assay in mice. Vascular permeability in the skin was assessed using the Miles assay[25,26]. Nine-week-old CD-1 female mice were injected with 100 μl PBS containing 1×10^6 colony-forming units (c.f.u.) of *B. anthracis* Sterne, ΔLF and ΔEF bacteria subcutaneously in the hind flank (three spots per mouse). After 6 h, mice were injected intravenously with 0.1 ml of 2% Evans blue in PBS and 30 min later mice were killed, skins were inverted and examined. For leakage quantification, the site of injection was excised and placed in formamide at 65 °C (24 h) for dye extraction (absorbance 620 nm). Statistical significance was assessed using one-way ANOVA.

31. Cook, O., Biehs, B. & Bier, E. *brinker* and *optomotor-blind* act coordinately to initiate development of the L5 wing vein primordium in *Drosophila*. *Development* **131,** 2113–2124 (2004).
32. Lunde, K. *et al.* Activation of the *knirps* locus links patterning to morphogenesis of the second wing vein in *Drosophila*. *Development* **130,** 235–248 (2003).
33. O'Neill, J. W. & Bier, E. Double-label *in situ* hybridization using biotin and digoxigenin-tagged RNA probes. *Biotechniques* **17,** 874–875 (1994).